

## Expression of *Oryza sativa* *OsSte12* transcription factor influencing antioxidant enzymes, sugar-related operons, and sugar metabolism in *Escherichia coli*

Kuan-Hung LIN<sup>1</sup>, Chih-Chun CHEN<sup>2</sup>, Shwu-Fen PAN<sup>2</sup>,  
Yu-Tsung LEE<sup>3</sup>, Minh Tan PHAM<sup>4</sup>, Chih-Ming CHIANG<sup>2\*</sup>

<sup>1</sup>Chinese Culture University, Department of Horticulture and Biotechnology, Taipei, 111, Taiwan; [rlin@ulive.pccu.edu.tw](mailto:rlin@ulive.pccu.edu.tw)

<sup>2</sup>Ming Chuan University, Department of Biotechnology, Taoyuan, 333,

Taiwan; [0988785395chen@gmail.com](mailto:0988785395chen@gmail.com); [sfpan@mail.mcu.edu.tw](mailto:sfpan@mail.mcu.edu.tw); [cmchiang@mail.mcu.edu.tw](mailto:cmchiang@mail.mcu.edu.tw) (\*corresponding author)

<sup>3</sup>Chang Gung University of Science and Technology, College of Human Ecology, Research Center for Food and Cosmetic Safety, Taoyuan, 333, Taiwan; [yilee@mail.cgu.edu.tw](mailto:yilee@mail.cgu.edu.tw)

<sup>4</sup>Ton Duc Thang University, Faculty of Applied Sciences, Ho Chi Minh city, 70000, Vietnam; [phamminhtan@tdtu.edu.vn](mailto:phamminhtan@tdtu.edu.vn)

### Abstract

Ste12 is a C2H2 zinc finger protein transcription factor involved with mating pheromones and regulating protein pathways in microorganisms. Previously, we isolated Ste12 cDNA from rice (*Oryza sativa*) involved with sugar starvation of  $\alpha$ -Amylase in seeds. In this study, we investigated how *OsSte12* regulated antioxidant enzymes, sugar-related operons, and sugar metabolism by over-expressing *OsSte12* in *Escherichia coli* via transformation. When transformed *OsSte12 E. coli* was grown in glucose and lactose media, it used these substrates and expressed more activity in ascorbate peroxidase, superoxide dismutase, and sucrose synthase compared to a non-transformant (NT) *E. coli* strain. Moreover, transformants could be grown in lactose for higher  $\beta$ -galactosidase activity than NTs or in mannitol. In lactose medium, highly-expressed RNA levels of *LacI* and *LacY* were found in transformants, while *LacZ* gene expression in transformants was significantly reduced compared to NTs. In sucrose and fructose media, *FruB* and *FruK* transcripts were both significantly higher in transformants than in NTs, whereas *FruA* transcripts did not show significant differences between transformants and NTs. Compared to NTs, *OsSte12* transcriptions of all transformants were significantly up-regulated in response to all sugar sources, but transformants were over-expressed more highly when was grown in lactose than in other sugars. Our results are important for elucidating the regulatory mechanisms of sugars and provide new insights into physiological relevance in *OsSte12* transformed *E. coli*.

**Keywords:** C2H2 zinc fingers; heterologous expressions; lactose; sugar metabolism

Received: 18 Oct 2025. Received in revised form: 14 Nov 2025. Accepted: 07 Dec 2025. Published online: 21 Dec 2025.

From Volume 49, Issue 1, 2021, Notulae Botanicae Horti Agrobotanici Cluj-Napoca journal uses article numbers in place of the traditional method of continuous pagination through the volume. The journal will continue to appear quarterly, as before, with four annual numbers.

## Introduction

Ste12, a C2H2 zinc finger protein transcription factor (TF), is involved with mating pheromones and the regulation of mitogen-activated protein kinase (MAPK) pathways in fungi or yeast, and also in control at the post-translational level via phosphorylation, protein stability, and protein–protein interactions (Madhani *et al.*, 1997; Hoi *et al.*, 2010; Wong and Dumas 2010; Gu *et al.*, 2015). In addition, Ste12 TF is also related to nutrient limitation, plant pathogenic virulence, dimorphic morphological transformation, and environmental adaptation (Elion *et al.*, 2005; Rispaill *et al.*, 2010; Asunción *et al.*, 2010; Merlin *et al.*, 2013; Wei *et al.*, 2017). *Cytospora chrysosperma* is the causal agent of poplar canker disease, and CcPmk1 (Fus3/Kss1) interacts with the downstream CcSte12 required for virulence in *C. chrysosperma* (Yu *et al.*, 2022); moreover, the CcPmk1-MAPK signaling pathway of *C. chrysosperma* recently reported to be involved with plant pathogenic fungi (Yu *et al.*, 2024). In *Trichoderma reesei*, Ste12 is involved in regulating cellulase gene expression grown on cellulose as a carbon source, utilization, and secondary metabolism (Schalamun *et al.*, 2024). Furthermore, Ste12 also affects the carbon source-dependent growth of *T. atroviride* (Gruber *et al.*, 2014). The *ste12-like* gene was involved in the regulation of abiotic stress tolerance in *Flammulina filiformis* in which the over-expression transformants were more tolerant to salt stress, cold stress, and oxidative stress than the non-transformants (Lyu *et al.*, 2023).

C2H2 zinc finger TF, Ros, which regulates both prokaryotic and eukaryotic promoters has been found in bacteria (Bouhouche *et al.*, 2000). The Ros protein of *Agrobacterium tumefaciens* has been reported to bind both bacterial and eukaryotic promoters (D’Abrosca *et al.*, 2020; Jia *et al.*, 2025), highlighting a rare but notable capacity for cross-domain transcriptional control. The first putative prokaryotic Cys2His2 zinc-finger domain has been identified in the transcriptional regulator Ros from *A. tumefaciens* (Malgieri *et al.*, 2007). The Cys2His2 zinc finger motif is essential for Ros DNA binding and is part of a larger DNA binding domain which includes four basic regions located on either side of the finger, one at the N-terminus and three at the C-terminus (Esposito *et al.*, 2006). C2H2 zinc-finger proteins form the largest family of DNA binding TFs coded by mammalian genomes, and there are twelve residues between the last zinc-coordinating cysteine and the first zinc-coordinating histidine found in a typical DNA-binding zinc-finger module (Zhang *et al.*, 2024). Furthermore, the Ros/MucR family of bacterial zinc-finger-containing proteins that integrate multiple functions, such as symbiosis, virulence, transcription regulation, motility, biosynthesis of surface components, biofilm formation, competitiveness, and various other physiological processes in cells (Janczarek *et al.*, 2022). This regulatory protein family is conserved in bacteria and is characterized by its zinc-finger motif, which has been proposed as the ancestral domain from which the eukaryotic C2H2 zinc-finger structure has evolved. However, the function and regulatory mechanisms of the Ste12 gene in *Escherichia coli* are still mysteries.

In the yeast *Saccharomyces diastaticus*, the STA1 gene encodes glucoamylase for degrading starch into glucose, and Ste12 activates the transcription of the STA1 gene in the absence of glucose (Kim *et al.*, 2004a). Furthermore, glucose-dependent repression of STA1 expression is imposed by Sfl1 transcriptional repressor, and Sfl1 prevents the binding to Ste12 required for STA1 expression (Kim *et al.*, 2004b). Tan *et al.* (2022) reports that the MAPK signal transduction cascade in yeast is highly up-regulated by several TFs, including the Ste12 gene under CO<sub>2</sub> sensing and CO<sub>2</sub>-induced metabolism. Previously, we found a sugar response sequence (SRS), containing three motifs, GC, G, and TATCCA elements, was the promoter of rice (*Oryza sativa* cv. TNG67)  $\alpha$ -amylase gene (*a-Amy3*), and has been shown to confer sugar responsiveness to a *CaMV35S* minimal promoter (Lu *et al.*, 1998). In addition, we also showed that *a-Amy3* promoter activity was suppressed by glucose using rice embryo transient assays (Lu *et al.*, 2002). We then isolated Ste12 from rice and found that the cDNA sequence of *OsSte12* (accession AK110102.1 in National Center for Biotechnology Information; <http://www.ncbi.nlm.nih.gov>) is a protein homologous to Ste12 in microorganisms. *OsSte12* played a crucial role in the sugar starvation of *a-Amy3* in isolated embryos using the gene gun transient assay (Appendix F1).

The aligns with recent systems-level observations that eukaryotic-like TFs can retain DNA-binding capacity in prokaryotic contexts, influencing local transcriptional machinery interactions (Lang *et al.*, 2024; Pinheiro *et al.*, 2025). Therefore, the characterization and functional analysis of the *OsSte12* gene should facilitate our understanding of the sugar response mechanism in *E. coli*. The objective of this investigation was to study how *OsSte12* influences sugar metabolism and signal transduction in *E. coli* by over-expressing *OsSte12* cDNA via transformation. We hypothesized that the over-expression of *OsSte12* in transformed *E. coli* would induce sugar metabolite expression and significantly increase the activity of antioxidant enzymes and sugar-related operons to elevate stress tolerance in comparison to a non-transformant *E. coli* (NT, vector only control) strain. Our transformed *E. coli* results are important for elucidating the regulatory mechanisms of sugars and provide a broad foundation for industrial fermentation, beverage, and diverse applications.

In our study, *OsSte12* expression in *E. coli* induced distinct transcriptional responses in sugar-metabolite and antioxidant enzyme genes, which may reflect the cross-domain compatibility of C2H2-type regulators with bacterial promoter structures, as previously noted for *Agrobacterium* Ros binding both bacterial and eukaryotic promoters (D'Ambrosca *et al.*, 2020; Jia *et al.*, 2025). Therefore, while no canonical *Ste12* homolog is present in *E. coli*, the bacterial Ros/MucR-type zinc-finger regulators represent the most evolutionarily and mechanistically comparable family. These proteins share structural homology, DNA-binding logic, and functional versatility, providing a plausible model for how *OsSte12* could exert transcriptional influence within the *E. coli* system.

## Materials and Methods

### *Plasmid construction and gene cloning*

An *OsSte12* clone was used as the parental strain in this study. *OsSte12* was amplified with a polymerase chain reaction (PCR) using paired degenerated primers (*OsSte12*-5F and -3R; Table 1), and distilled-deionized water (dd H<sub>2</sub>O) was used as a negative control. The *OsSte12* fragment was amplified as 1,260 bp. PCR products were purified using the SNAP Gel Purification Kit (Thermo Fisher Scientific, Waltham, MA, USA). Purified DNA was ligated to the destination vector pET-61-DEST (Novo ProBioscience, Shanghai, China), yielding the strain pET-61-DEST/*OsSTE12* (Appendix F2) using the pENTR™/D-TOPO™ Cloning Kit (Thermo Fisher). The strain was then transformed into *E. coli* strain DH5 $\alpha$  (Yi-Shan Biotech, Taipei, Taiwan) maintained on Luria–Bertani (LB) medium (0.5% yeast extract, 1% bacto-tryptone, and 1% NaCl) at 37 °C. The pENTR™/D-TOPO™ system was separated into two parts for pENTR™ TOPO cloning and a Gateway LR Clonase enzyme mixed (LR) exchange reaction for the destination vector (Lin *et al.* 2019). After ampicillin (100  $\mu$ g/ml) selective screening of the colony, plasmid insertion *OsSte12* was confirmed by PCR in an Eppendorf Mastercycler Gradient Thermal Cycler (Hamburg, Germany) with the following thermal program: initial denaturation at 94 °C for 5 min, followed by 30 cycles at 94 °C for 1 min, 55 °C for 30 s, and 72 °C for 1 min, with a final extension at 72 °C for 10 min. The products were electrophoretically separated on 1.5% agarose gel, and the predicted size of 1,260 bp of the *OsSte12* gene (accession no. AK110102) was verified with a 1,000bp DNA ladder marker. The recombinational cloned *E. coli* strain BL21 (DE3, vector-only, non-transformant, NT) was confirmed by PCR using the His-*OsSte12* paired primer (Table 1), and the products were sent to Genomics Biotech (Taipei, Taiwan) for sequencing and data analysis. Gene sequences were then compared with other species using the NCBI-BLAST database (<https://blast.ncbi.nlm.nih.gov/Blast.cgi>).

**Table 1.** Paired primers used in the study

Name	Sequence	Expected size (bp)
<i>OsSte12</i>	F : 5'-CACCATGTCAATGCCTCCT3'	1,260
	R : 5'-TCAGTAGTGGCTGGC-3'	
<i>His-OsSte12</i>	F : 5'-CACCACCACCACTCCATCAT-3'	280
	R : 5'-CGAGTCAAACCACAACCTCGC-3'	
<i>bglB</i>	F : 5'-TCGATGACCGCTCGATTAGC-3'	149
	R : 5'-ACCGAATGAAGCGGGGTTAG-3'	
<i>bglF</i>	F : 5'-CTAACCCCGCTTCATTTCGGT-3'	186
	R : 5'-GGAAAAATGGAACCGCGCAT-3'	
<i>LacI</i>	F : 5'-TCGTCGTATCCCCTACCCT-3'	144
	R : 5'-AGTGCCATGTCCGGTTTTCA-3'	
<i>LacY</i>	F : 5'-TTACTGCGACGGCTGACTTT-3'	138
	R : 5'-GTGATGTTTTCGCGCGTTCTT-3'	
<i>LacZ</i>	F : 5'-TAGATGGGCGCATCGTAACC-3'	230
	R : 5'-AAAACCCCTGGCGTTACCCAA-3'	
<i>FruA</i>	F : 5'-TGTCAGTACACATCATGCCA-3'	203
	R : 5'-AACTGCCACAGAGTATGGAG-3'	
<i>FruB</i>	F : 5'-TCTGCTTTTCGCCCATCAGT-3'	152
	R : 5'-CGTGGCAATCGGTATTGCTG-3'	
<i>FruK</i>	F : 5'-CTTCCGCTGACACAGACCAT-3'	166
	R : 5'-CATTGCCAACCGTTTCCAGG-3'	
<i>gyrA</i>	F : 5'-GTCGTGGCGGAAAGGTAAA-3'	132
	R : 5'-CGGCTGGAGAAGCACAGAA-3'	

*Phylogenetic analysis of OsSte12 in E. coli*

The full-length 419 amino acid sequences of Ste12 proteins from *Oryza sativa japonica* (AK110102) and their orthologs in *Alternaria alternata* (XM\_018535684.1), *A. burnsii* (XM\_038935594.1), *A. atra* (XM\_043319471.1), *A. arborescens* (XM\_028654211.1), *A. solani* (CP\_022030.1), *A. rosae* (XM\_046165985.1), *Pyrenophora tritici* (XM\_001931393.1), *Bipolariszeicola* (XM\_007709410.1), *B. maydis* (XM\_014220977.1), *B. sorokiniana* (XM\_007699120.1), *B. oryza* (XM\_007688094.1), *B. victoriae* (XM\_014704489.1), *Dothidotthia symphoricarpi* (XM\_033670547.1), *Exserohilum turcica* (XM\_008024982.1), *Cucurbitaria berberidis* (XM\_040927895.1), *Ascochyta rabiel* (XM\_038937715.1), *Didymella exigua* (XM\_033590852.1), *Marcoventuria anomochaeta* (XM\_033709499.1), *Boeremia exgua* (XM\_046139244.1), and *Leptosphaeria maculans* (Fo\_906023.1) were aligned with ClustalX (Larkin *et al.*, 2007). Sequences of these 21 deduced proteins were downloaded from NCBI with GenBank numbers, and predicted conserved domains/motifs were examined with Blast searches at NCBI. The MEGA 11 software package with default parameter settings was used to construct a neighbor-joining tree, with 1,000 bootstrap replications to evaluate clade support (Tamura *et al.*, 2021).

*Similarity of C2H2 domains between Oryza sativa and MucR/Ros genes from Rhizobiaceae family*

Two C2H2 zinc finger domains from *Oryza sativa* OsSte12(AK110102) were compared to homologous regions in MucR/Ros-family proteins from *Sinorhizobium fredii* (AWI62033), *Rhizobium leguminosarum* (AAT92553), *Rhizobium etli* (AAC44878), and *A. tumefaciens* (WP\_132517515.1). Protein sequences were retrieved from NCBI and aligned using BLASTp (v2.12.0) with the BLOSUM62 matrix (Altschul *et al.*, 1997). To improve sensitivity in detecting remote homologs, structural alignments were also

performed using DeepBLAST, a deep learning-based method for predicting structure-informed alignments from sequence alone (Hamamsy *et al.*, 2024) and HHblits, which employs HMM–HMM profile alignment (Remmert *et al.*, 2012). Sequence similarity was further evaluated using ProtSub, a substitution matrix optimized for detecting distant functional relationships (Garg *et al.*, 2025). All alignments were manually curated to ensure conservation within the C2H2 domain boundaries.

#### *Analysis of E. coli strain growth rate on different kinds of sugar agents*

Cell culturing of both pET-61-DEST/*OsSte12* clones and NT BL21 (DE3) (as control) was carried out in 5 ml of LB medium (bacto-tryptone 10 g L<sup>-1</sup>, yeast extract 5 g L<sup>-1</sup>, and NaCl 10 g L<sup>-1</sup>; for solid medium, agar 15 g L<sup>-1</sup> was added, and pH adjusted to 7.0 before autoclaving/ with 100 µg mL<sup>-1</sup> of ampicillin) to optical density at 600 nm (OD<sub>600</sub>) of 0.8-1.0. After then, adding 1 mL of it to 50 mL of sugar-base medium (containing 100 mM of lactose, sucrose, glucose, fructose, or mannitol) in 0.1% yeast extract (Bernaerts and De Ley, 1963) to observe the growth of transformed *OsSte12* and NT *E. coli*. *E. coli* growth rates were recorded in 20 min intervals for 3 h using an Elisa reader (Spectra MAX 190, Molecular Devices, USA). Relative growth values from 0 min (blank) to 180 min were calculated using the coefficient of the linear regression of the curve representing OD<sub>600</sub> versus time as previously described (Sezonov *et al.*, 2007). All bacterial strains were cultured under standard conditions at 37 °C with shaking 200 rpm (Subramanian *et al.*, 2024).

#### *Protein extraction and determination of enzyme activity*

For enzyme assays, both *E. coli* BL21 (DE3)/pET-61-DEST (vector-only control, NT) and BL21 (DE3)/pET-61-DEST/*OsSte12* transformants (recombinant strain) were cultured in 50 ml of M9 minimal medium (Na<sub>2</sub>HPO<sub>4</sub> 6.78 g L<sup>-1</sup>, KH<sub>2</sub>PO<sub>4</sub> 3.0 g L<sup>-1</sup>, NaCl 0.5 g L<sup>-1</sup>, NH<sub>4</sub>Cl 1.0 g L<sup>-1</sup>, MgSO<sub>4</sub> 0.24 g L<sup>-1</sup>, and CaCl<sub>2</sub> 0.01 g L<sup>-1</sup>) supplemented with 0.4% (w/v) glucose, sucrose, fructose, lactose, mannitol, and in sugar-free control medium. Cells were harvested after 4 h of IPTG induction (0.5 mM, 37 °C, 200 rpm). Cell pellets were washed twice with 50 mM phosphate buffer (pH 7.0) and resuspended in extraction buffer (50 mM phosphate buffer, 1 mM EDTA, 1 mM DTT). The suspension was sonicated and centrifuged (12,000 *xg*, 4 °C, 15 min) to obtain the crude enzyme extract, and quantified with a Bradford Protein Assay Kit (BioRad, Hercules, CA, USA).

Protein samples from each sugar substrate treatment were prepared for the activity analyses of superoxide dismutase (SOD, EC 1.15.1.1), glutathione reductase (GR, EC 1.6.4.2), ascorbate peroxidase (APX, EC 1.11.1.11), sucrose synthase (SUS, EC 2.4.1.13), and β-galactosidase (EC 3.2.1.23). For SOD activity measurement, the extraction buffer, reaction mixture, and activity calculation were executed using protocols described by Hemmadi (2016). GR activity was determined by the GSH dependent oxidation of NADPH according to Engström-Öst *et al.* (2019). APX activity was assessed by measuring the initial rate of disappearance of ascorbate following Gomes *et al.* (2022). The HCL-resocinol method was used for SUS activity measurement, adopted from Ren *et al.* (2020). Lastly, the O-nitrophenyl-beta-D-galactopyranoside (ONPG)-Na<sub>2</sub>CO<sub>3</sub> method was used to determine β-galactosidase activity as described previously (Lu *et al.*, 2007).

#### *Western blot analysis*

Fifty micrograms of total protein from each sample of *OsSte12* transformant and NT were loaded into a 5% stacking gel and 10% resolving gel (sodium dodecyl sulfate polyacrylamide gel electrophoresis; SDS-PAGE), and electrophoresis performed at 250 V with 20 mA for 2 h on Mini PROTEAN III equipment (BioRad). Following electrophoresis, proteins on gel were transferred to an Immobilon-P transfer membrane (Millipore, Billerica, MA, USA). The membrane was incubated at 4 °C overnight with a mouse anti-His antibody (Catalog # MA1-21315, Invitrogen) and anti-β-actin antibody (Catalog # mAbcam8226, Abcam).

Bands were detected with anti-mouse immunoglobulin G (IgG) peroxidase-conjugated secondary antibody for 2 h. Labels were detected with an immune-blot assay enhanced chemiluminescence (ECL) Kit (Pharmacia, Stockholm, Sweden) according to the manufacturer's instructions. The band intensity of His-OsSte12 in the photographed samples was analyzed using ImageJ software (Schneider *et al.*, 2012).

#### *Amplification of cDNA and expression analysis of sugar-metabolite genes*

One-and-a-half milliliters of sugar-base medium with transformed *E. coli* samples from each sugar substrate treatment were purified by centrifugation at 12,000xg, and supernatants were used for total RNA isolation using a NucleoZOL Kit (MACHEREY-NAGEL, Dueren, Germany). Total RNA was isolated from both *E. coli* BL21 (DE3)/pET-61-DEST (vector-only control) and BL21 (DE3)/pET-61-DEST/*OsSte12* transformants cultured in media containing different carbon sources (glucose, sucrose, fructose, lactose, and mannitol). RNA integrity was verified by agarose-gel electrophoresis and purity confirmed by  $A_{260}/A_{280}$  ratios of 1.9 - 2.1. Complementary (c)DNA was extracted from total RNA with a MMLV Reverse Transcription Kit (Promega Corporation, WI, USA) according to vendor instructions. Paired degenerated specific primers for *OsSte12*, *bglB* ( $\beta$ -glucoside operon), *bglF* ( $\beta$ -glucoside operon), *LacI* (lactose operon), *LacY* (lactose operon), *LacZ* (lactose operon), *FruA* [fructose-specific PTS (phospho-transferase system) multiphosphoryl transfer protein FruA], *FruB* (fructose-specific PTS multiphosphoryltransfer protein FruB), and *FruK* (1-phosphofructokinase) from the genome of *E. coli* (accession NC000913.3) were used for amplification (Table 1). PCR was carried out with the following thermal program: initial denaturation at 94 °C for 10 min, followed by 30 cycles each at 94 °C for 30 s, 55 °C for 30 s, and 72 °C for 1 min, with a final extension at 72 °C for 10 min. The products were electrophoretically separated on 1.5% agarose gels, and the predicted sizes of 280, 149, 186, 144, 138, 230, 203, 152, 166, and 132 bp from *OsSte12*, *bglB*, *bglF*, *LacI*, *LacY*, *LacZ*, *FruA*, *FruB*, *FruK* and *gyrA*, respectively (Table 1), were verified with 100 bp and 1 Kb DNA ladder markers.

To investigate whether *OsSte12* gene expression influenced the expression of sugar metabolic genes involved in the signal transduction pathways in the NT and transformant, the expression levels of sugar metabolic responsive genes were evaluated. The relative changes in *Ste12*, *bglB*, *bglF*, *LacI*, *LacY*, *LacZ*, *FruA*, *FruB*, and *FruK* gene expressions in response to the NT and transformant were monitored by quantitative real-time PCR (qRT-PCR) and quantification of RNA levels. A qRT-PCR was performed using a qPCR machine (MyGo PCR, Raynham, Massachusetts, USA). Reaction mixtures included 0.8  $\mu$ L of 10  $\mu$ M of each primer (Table 1), 10  $\mu$ L of 2  $\times$  qPCR-BIOSyGreen Mix (PCR Biosystem, London, UK), 2  $\mu$ L of cDNA template, and 10  $\mu$ L of ddH<sub>2</sub>O (20  $\mu$ L volume in total) for qRT-PCR. Thermal cycling conditions were as follows: 2 min at 95 °C, followed by 45 cycles of 5 s each at 95 °C and 30 s at 60 °C. To normalize the total amount of cDNA in each reaction, DNA gyrase subunit A (*gyrA*) from *E. coli* (accession NC\_000913.3; Liu *et al.*, 2022) was co-amplified as an internal control. The relative amount of RNA of each gene was calculated as the ratio of the transcription level between *OsSte12* and the NT by  $2^{-\Delta\Delta CT}$  method. All reactions were run in three replicates to ensure reproducibility, as recommended by Bustin *et al.* (2009) and Taylor *et al.* (2010).

#### *Statistical analysis*

Each NT and transformed *E. coli* with three replications was examined to determine RNA and protein levels, and enzyme activity. Data are presented as mean values of three independent sets of experiments with similar results. A paired Student's *t*-test was calculated with the least significant difference (LSD) at  $p < 0.05$  using SAS program ver. 9 (SAS Institute, Cary, NC, USA).

## Results

### *Phylogenetic analysis of OsSte12*

The 1,260bp coding sequence of *OsSte12* gene encodes a protein with 419 amino acid residues. The *OsSte12* protein shares 42-58% amino acid sequence identity and 61-74% sequence similarity with *Ste12*-like transcription factors from fungal species, such as *Trichoderma reesei*, *Alternaria alternata*, and *Magnaporthe oryzae*, suggesting an evolutionarily conserved DNA-binding architecture and functional analogy within the C2H2-type zinc-finger family that may underlie its ability to interact with *Ste12*-like promoter motifs even in heterologous bacterial contexts.

Twenty-one deduced *Ste12* conserved amino acid sequences were aligned and compared, and phylogenetic analysis show that *OsSte12* clustered with *A. alternate* and *Leptosphaeria maculans* (FO\_906023.1) *STE* domain mRNA in the sequence (Appendix F4). Identity among *OsSte12*, *A. alternata*, and *L. maculans* are 99% and 79%, respectively. Phylogenetic analysis of 17 representative *Ste12* sequences revealed clustering into distinct fungal lineages corresponding to *Alternaria*, *Bipolaris*, *Pyrenophora*, *Dothidotthia*, *Exserohilum*, *Cucurbitaria*, *Ascochyta*, *Didymella*, *Macroventuria*, *Boeremia*, and *Leptosphaeria*, all within the Pleosporales order of Dothideomycetes. These results align with previous reports on *Ste12* orthologs regulating fungal morphogenesis and MAPK-dependent pathogenicity (Rispaill *et al.*, 2010; Yu *et al.*, 2022; Schalamun *et al.*, 2024). Although phylogenetically distinct, the rice *OsSte12* retains canonical C2H2 zinc-finger motifs (CPIPTCGRLFKRLEHLKRHVRTH and CPLCNKAFSRSDNLAQHRRTH), suggesting early diversification from a common ancestral C2H2-type regulator shared by plants and fungi (Zhang *et al.*, 2024). Comparative modeling (Zhang *et al.*, 2024; Lang *et al.*, 2024) indicates that *OsSte12* preserves the  $\beta\beta\alpha$ -fold and Cys-His coordination essential for promoter binding, supporting structural convergence with fungal *Ste12* proteins. This conservation underscores the evolutionary continuity of MAPK-responsive C2H2 regulators and their diversification into phylogenetically distinct transcriptional networks (Rispaill and Di Pietro, 2010; Pinheiro *et al.*, 2025).

### *Sugar-induced expression of OsSte12 in E. coli*

The N-terminal of the *OsSte12* plasmid was fused with a polyhistidine-tag (6xHis) (Appendix F2) and transformed into the *E. coli* strain to detect the expression of the *OsSte12* gene, and the transformants were grown in sugar and no-sugar media. Western blot analysis was conducted followed by using antiserum anti-His to identify *OsSte12* expression. Figure 1 shows that relative amounts of the 6xHis proteins accumulated in all transformants with a clear 6xHis band displaying 43KDa, and were significantly induced in glucose, sucrose, lactose, and fructose media with 2.0, 2.3, 2.6, and 4.3 fold, respectively, compared to no-sugar cultures. Transformants cultured with the fructose medium showed substantially higher His-*OsSte12* accumulation than with other media. However, no His-*OsSte12* band was displayed in the NT.  $\beta$ -actin, a housekeeping gene consistently expressed in *E. coli*, was used as an internal control.

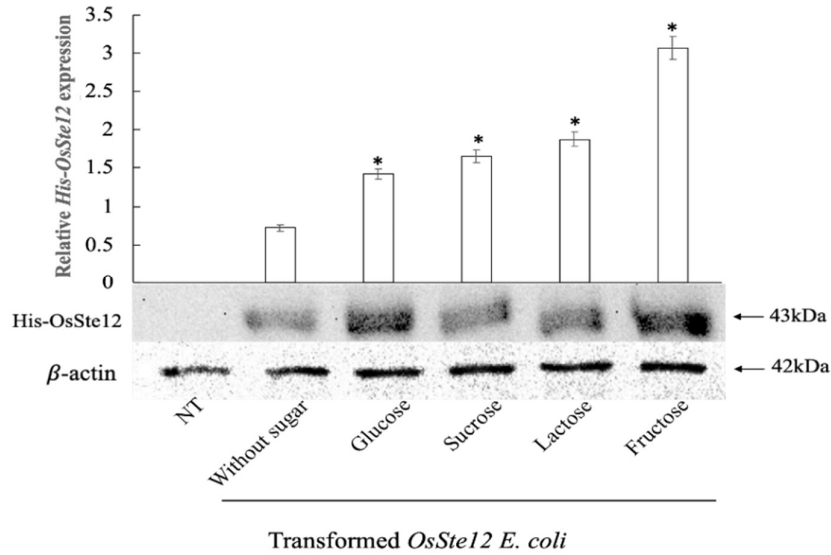
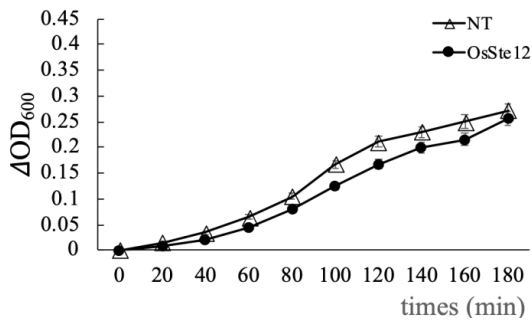


**Figure 1.** Western blot analysis of transformed *OsSte12 E. coli* and NT strain BL21 (DE3) *OsSte12* was cultured in LB broth containing no-sugar medium and 100 mM of glucose, sucrose, lactose, or fructose. Fifty micrograms of total protein in each sample from the *OsSte12* transformant and NT were used for each sample. The  $\beta$ -actin was used as an internal control, in which exhibited in all samples at 42KDa is indicated by an arrow. The molecular weight of His-OsSte12 at 43KDa is indicated by an arrow. The band intensity of His-OsSte12 in the photographed sample was analyzed using Image J software. Error bars indicate the standard deviation (SD) from the means of triplicate samples. Asterisks indicate significant differences ( $p \leq 0.05$ ) between each sugar and no-sugar media in transformants

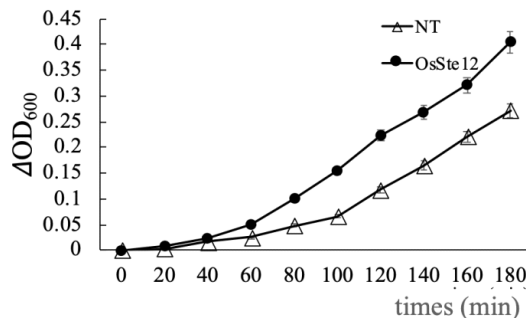
*Lactose media strongly promotes strain growth*

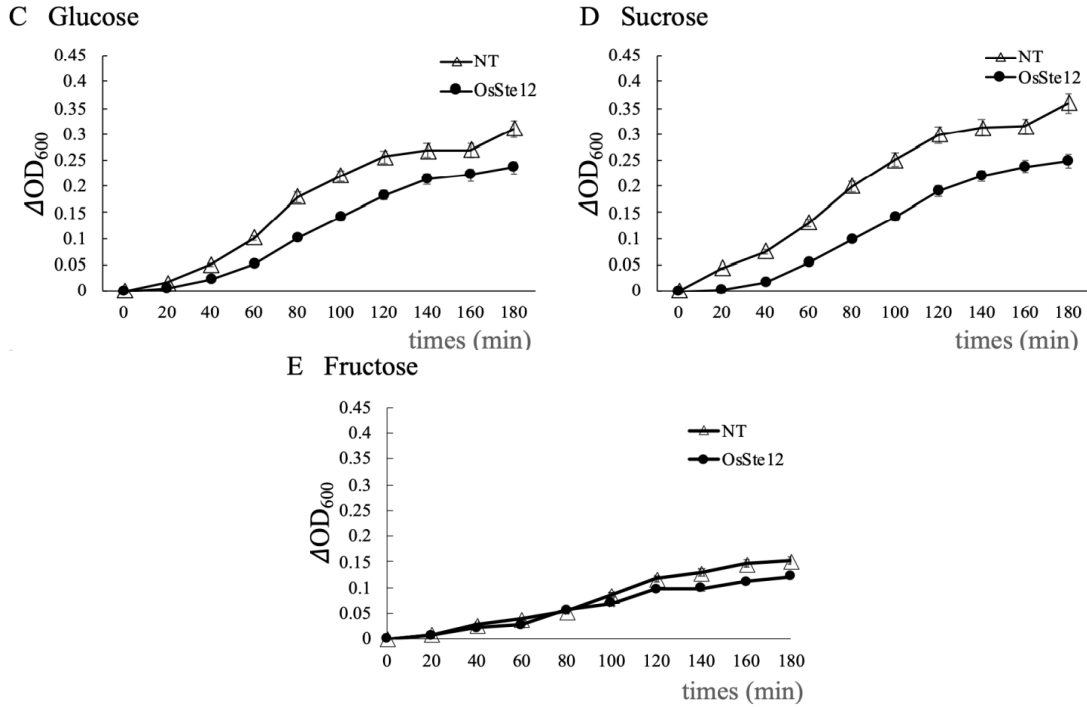
The abilities of the transformed *OsSte12* strain and NT plasmid grown on various sugar substrates were assessed over a 3 h period of growth change (Figure 2). All sugars enabled growth in the transformed and NT *E. coli* strains, and growth rates were elevated as time increased, reaching their highest production at 3 h after culture initiation. All transformants grown on glucose, sucrose, fructose, and no-sugar media showed remarkably reduced growth time periods compared to NT (Figures 2A, C, D, and E). Nevertheless, transformant growth on lactose showed significantly higher growth rates from 1.35- to 2.33- fold after 20 min to 3 h culturing compared to NT (Figure 2B).

**A Without sugar**



**B Lactose**

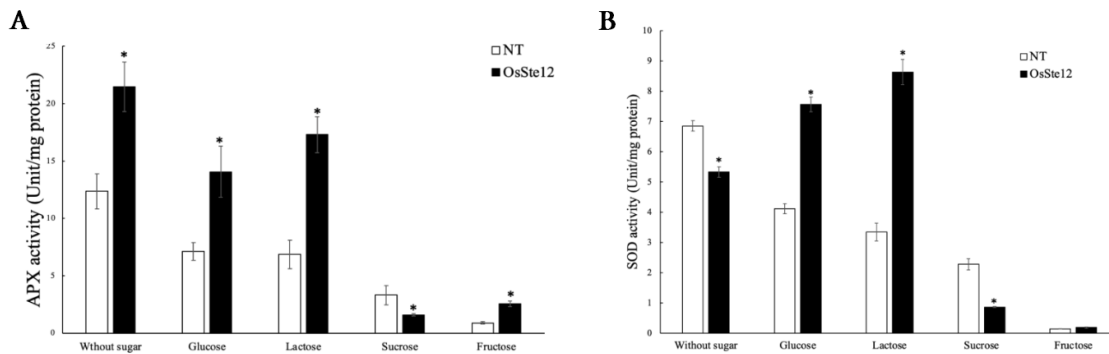




**Figure 2.** Cell cultures of transformed and NT *OsSte12 E. coli* strains were cultured in LB broth containing no-sugar medium (A) and 100 mM of lactose (B), glucose (C), sucrose (D), and fructose (F) to observe growth rates in *OsSte12 E. coli* (circle) and NT strains (triangle) recorded in 20 min intervals for 3 h. Relative growth values from 0 min (blank) to 180 min were calculated using the coefficient of the linear regression of the curve representing OD<sub>600</sub> versus time. Error bars indicate standard deviations (SD) from means of triplicate samples. A paired Student's *t*-test was calculated with the least significant difference (LSD) at *p* < 0.05

*Sugar types and sugar-free media significantly impact transgenic cell enzyme activity*

Enzyme activity measurements revealed that *OsSte12* expression markedly influenced antioxidant metabolism depending on the carbon source. In Figure 3A, APX activity in all transformants grown in sugar and no-sugar media was significantly higher than in NT cells, except that transformants grown in sucrose had significantly lower APX activity compared to NT. In Figure 3B, compared to NT, SOD activity was significantly higher in transformants in glucose and lactose media with 2.1 and 2.7 fold, respectively, but lower in transformants in sucrose and no-sugar media. However, no discernible difference in SOD activity was observed between NT and transformants in the fructose medium. Interestingly, GR activity in all transformants subjected to sugar and no-sugar media was significantly lower than in NT strains (Figure 3C).



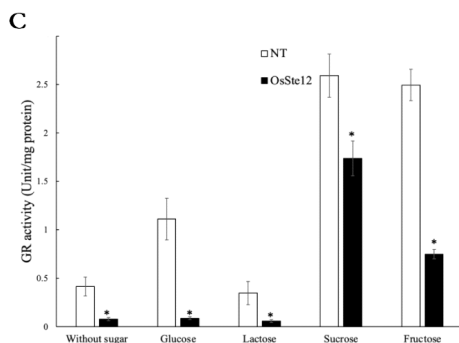


**Figure 3.** Comparisons between transformed and NT *OsSte12 E. coli* strains cultured in sugar-base medium containing no-sugar and 100 mM of glucose, lactose, sucrose, and fructose. Protein samples from each sugar substrate treatment were prepared for the activity (U/mg protein) analyses of APX (A), SOD (B), and GR (C)

Error bars indicate standard deviations (SD) from means of triplicate samples. Asterisks indicate significant differences ( $p \leq 0.05$ ) between transformed *OsSte12 E. coli* and NT strains

Significantly increased SUS activity was displayed in transformants grown in glucose and lactose media with 1.9 and 3.9 fold, respectively, compared to NT, while significantly decreased SUS activity was found in transformants grown in sucrose, fructose and no-sugar media compared to NTs (Figure 4A). All transformants under lactose culture had significantly higher  $\beta$ -galactosidase activity than in mannitol and all NT cells in lactose and mannitol (Figure 4B). No significant  $\beta$ -galactosidase activity changes were observed among all NT cells under lactose and mannitol culture media. Remarkable reductions of  $\beta$ -galactosidase activity were observed in all transformants subjected to the mannitol medium. In addition, the highest  $\beta$ -galactosidase activity (345.12 U/mg protein) was observed in transformants under 20 mM lactose medium compared to other concentrations.

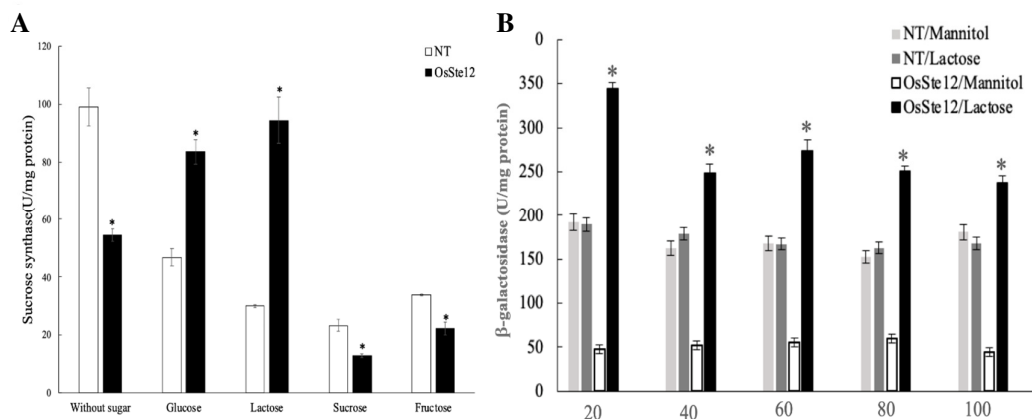


**Figure 4.** Comparisons between transformed and NT *OsSte12 E. coli* strains cultured in sugar-base medium containing no-sugar and 100 mM of glucose, lactose, sucrose, and fructose for sucrose synthase activity (U/mg protein) analysis (A). Comparisons between transformed and NT *OsSte12 E. coli* strains cultured in LB broth containing 20, 40, 60, 80, and 100 mM of mannitol and lactose for  $\beta$ -galactosidase activity (U/mg protein) analysis (B)

Error bars indicate standard deviations (SD) from means of triplicate samples. Asterisks indicate significant differences ( $p \leq 0.05$ ) between transformed *OsSte12 E. coli* and NT strains

*Quantitative expression profiling of transformants via qRT-PCR*

Transcript levels of sugar metabolite genes were analyzed to verify whether these gene expressions corresponding to functions generated by the *OsSte12* gene were expressed in transformants and NTs. Putative *OsSte12* transformant *E. coli* was screened by RT-PCR assays with degenerated primer pairs (Table 1), the results showing that *bglB*, *bglF*, *LacI*, *LacY*, *LacZ*, *FruA*, *FruB*, and *FruK* cDNA fragments were expressed in the transformants and NTs (Figure 5A). The *gyrA* from *E. coli* was used as an internal control, and transcripts were exhibited in all samples. Various transcript levels were observed, and RNA abundances of all sugar metabolite genes in transformants were significantly up-regulated and higher than their NTs, except for *LacZ* and *FruA* (Figure 5B). *OsSte12* transcription in NTs was non-detectable due to the His-*Oste12* specific paired primer (Table 1) being used to amplify *OsSte12*.

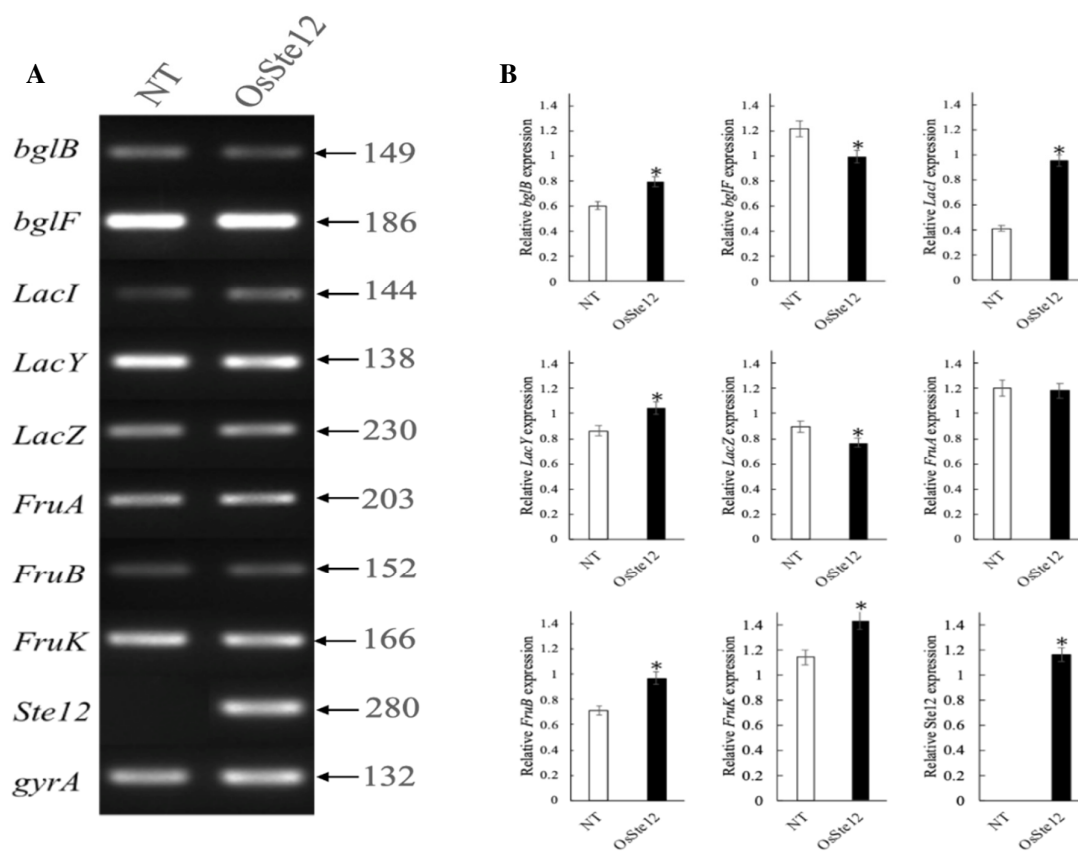


**Figure 5.** Amplification of cDNA fragments from sugar metabolite genes, *bglB*, *bglF*, *LacI*, *LacY*, *LacZ*, *FruA*, *FruB*, *FruK*, and *Ste12* by reverse transcription (RT)-PCR analysis in transformed and NT *OsSte12 E. coli* strains

Total RNA in all tested samples was extracted from *OsSte12* transformant and NT treatments with 100 mM each of glucose, sucrose, lactose, and fructose. The expected sizes of *bglB*, *bglF*, *LacI*, *LacY*, *LacZ*, *FruA*, *FruB*, *FruK*, *Ste12*, and *gyrA* at 149, 186, 144, 138, 230, 203, 152, 166, 280 and 132 bp, respectively, are indicated by an arrow (A). The *gyrA* from *E. coli* was used as an internal control, and transcripts were exhibited in all samples. The relative expression level of each sugar metabolite gene was compared between transformant and NT strains (B). Error bars indicate standard deviations (SD) from means of triplicate samples. Asterisks indicate significant differences ( $p \leq 0.05$ ) between transformed *OsSte12 E. coli* and NT strains

Transformants were then confirmed by qRT-PCR analysis to check the effects of sugar metabolite gene expression on transformants and NTs grown in various sugar media. Both *bglB* and *bglF* expressions were unaffected in transformants and NTs under the glucose culture medium (Figure 6A). Both *LacI* and *LacY* expressions were significantly up-regulated in transformants compared to NTs in the lactose culture medium, whereas *lacZ* expression in transformants was down-regulated and obviously lower than in NTs (Figure 6B). In sucrose and fructose media, transcript levels of both *FruB* and *FruK* were significantly higher in transformants than in NTs, whereas *FruA* transcripts did not show significant differences between transformants and NTs (Figures 6C and D).

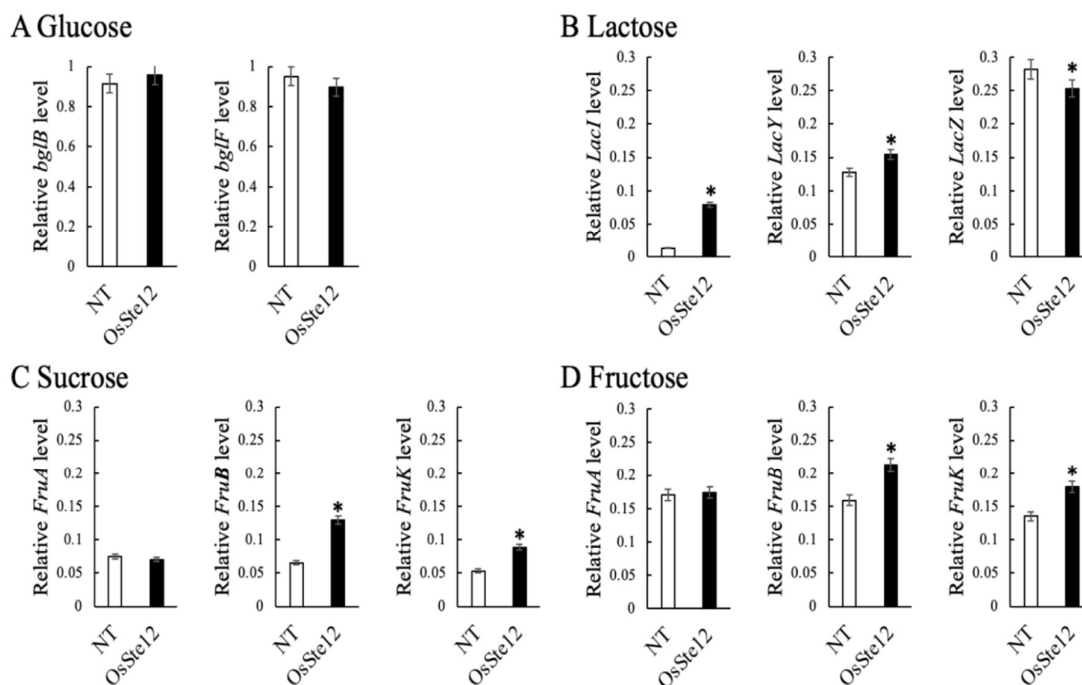


**Figure 6.** Relative RNA levels in *bglB*, *bglF*, *LacI*, *LacY*, *LacZ*, *FruA*, *FruB*, and *FruK* gene expressions in response to NTs and transformants cultured in glucose (A), lactose (B), sucrose (C), and fructose (D) media were monitored by quantitative real-time PCR (qRT-PCR)

To normalize the total amount of cDNA in each reaction, *gyrA* from *E. coli* (accession NC\_000913.3) was co-amplified as an internal control. The relative amounts of RNA of each gene were calculated as the ratio of the transcription levels between the *OsSte12* strain and its NT by the  $2^{-\Delta\Delta CT}$  method. Error bars indicate standard deviations (SD) from means of triplicate samples. Asterisks indicate significant differences ( $p \leq 0.05$ ) between transformed *OsSte12 E. coli* and NT strains

As shown in Figure 7, *Ste12* transcriptions of all transformants were significantly up-regulated in response to different sugar sources compared to NTs (trace amounts to non-detectable), and a higher over-expressed transformant was grown in lactose than other sugars.

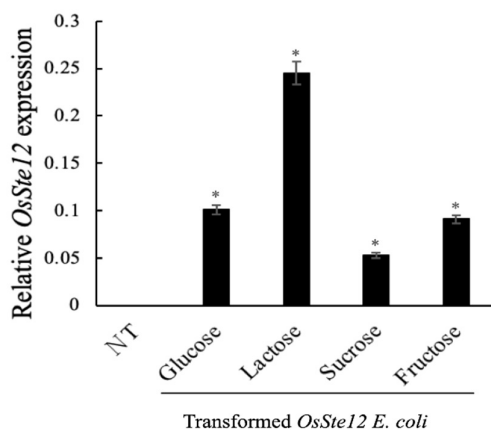


**Figure 7.** Relative *OsSte12* transcriptions of all transformants in response to glucose, lactose, sucrose, and fructose compared to NTs

Error bars indicate standard deviations (SD) from means of triplicate samples. Asterisks indicate a significant difference ( $p \leq 0.05$ ) between transformed *OsSte12 E. coli* and NT strains

#### Similarity of C2H2 domains

The structural analysis identified two putative C2H2-type zinc finger motifs in *OsSte12* (Table 2). These domains share notable similarity with zinc finger motifs of bacterial Ros/MucR-type regulators. Specifically, the C2H2\_1 domain (CPIPTCGRLFKRLEHLKRHVTRTH) shares 34.78% identity with sequences from *A. tumefaciens* and *Rhizobium* spp., while the second domain C2H2\_2 (CPLCNKAFSRSDNLAQHRRTH) though less conserved (23.81%), groups phylogenetically with the Ros/MucR family.

**Table 2.** Similarity of C2H2 Domains between *Oryza Sativa* and MucR/Ros genes from *Rhizobiaceae* family

Target domain	Sequence ID	Best matching region	Similarity (%)
C2H2_1	<i>OsSte12</i> (AK110102)	CPIPTCGRLFKRLEHLKRHVTRTH	100.0
C2H2_1	<i>MucR1</i> (AWI62033)	NDQITCLECGGAFKSLKRHLMTH	34.78
C2H2_1	<i>RosR</i> (AAT92553)	DEQITCLECGGNFKSLKRHLMTH	34.78
C2H2_1	<i>Ros</i> (AAC44878)	DEQITCLECGGNFKSLKRHLMTH	34.78
C2H2_1	<i>Ros</i> (WP_132517515.1)	DDQITCLECGGSFKSLKRHLMTH	34.78
C2H2_2	<i>OsSte12</i> (AK110102)	CPLCNKAFSRSDNLAQHRRTH	100.0
C2H2_2	<i>MucR1</i> (AWI62033)	QITCLECGGAFKSLKRHLMTH	23.81
C2H2_2	<i>RosR</i> (AAT92553)	VPVSDLANLISDVHSALSNTS	23.81
C2H2_2	<i>Ros</i> (AAC44878)	VPVSDLANLISDVHSALSNTS	23.81
C2H2_2	<i>Ros</i> (WP_132517515.1)	QITCLECGGSFKSLKRHLMTH	23.81

The *OsSte12* protein from *Oryza sativa* (AK110102) was subjected to comparative analysis with homologous sequences from *Sinorhizobium fredii* CCBAU 4546 (AWI62033), *Rhizobium Leguminosarum* (AAT92553), *Rhizobium etli* (AAC44878), and *Agrobacterium tumefaciens* (WP\_132517515.1)

## Discussion

When transformed *E. coli* strain *OsSte12* was cultured in glucose, fructose, lactose, and sucrose as preferred and sequential sugar sources, lactose was used and triggered the highest growth rate among the sugar substrates and their NT plasmids (Figure 2). Growth duration of transformants and NTs lasted for more than

3 h in all sugar and non-sugar (control) media. Transformed *OsSte12* plasmid was probably constructed with the Lac promoter, and resulted in higher catabolite lactose than other sugars. Over-expression in transformants (Figures 5B and 6B) may induce higher growth rates in *E. coli* strains grown on lactose than other sugar substrates. We also speculate that sequential consumption of lactose is an adaptation for rapidly consuming the most beneficial substrate for transformants (Aidelberg *et al.*, 2014). On the other hand, the 100 mM sucrose, glucose, and fructose concentrations were too high to grow transformants due to their osmotic-caused stress environments (Record *et al.*, 1998). Further work is needed to explore the potential of *OsSte12* adaptation and tolerance at the gene regulatory level.

When transformed *OsSte12* was grown in glucose and lactose, it used these substrates and accumulated more activity in APX, SOD, and SUS compared to NTs, while transformants exhibited significant catabolite repression of sucrose and prevented APX, SOD, GR, and SUS activity in comparison to NTs (Figures 3 and 4A). The level of fructose-induced APX in transformants was significantly higher than in NTs, while the levels of fructose-induced GR and SUS in transformants were significantly lower than in NTs, and no significant differences were observed in SOD activity between transformants and NTs treated with fructose. Sucrose ( $\alpha$ -D-glucopyranosyl  $\beta$ -D-fructofuranoside) is cleaved to make glucose and fructose available for energy gaining reactions and macromolecule and amino acid biosynthesis. This reaction can be performed by enzymes, including SUS (Vargas *et al.*, 2008). These transformants maintain their ability to degrade stored sugars and mobilize it for enzyme activities. In addition, transformants can be grown in lactose for higher  $\beta$ -galactosidase activity than in mannitol and NT groups; moreover, during growth on mannitol and lactose, the concentration of these two substrates can be as low as 20 mM to accumulate  $\beta$ -galactosidase (Figure 4B). Mannitol was used as a control to rule out the influence of  $\beta$ -galactosidase from osmotic stress.  $\beta$ -galactosidase not only cleaves the disaccharide lactose to form glucose and galactose for glycolysis, but also catalyzes the transgalactosylation of lactose to allolactose. Allolactose can be cleaved to monosaccharides and binds to the *lacZ* repressor, creating the positive feedback loop that regulates the amount of  $\beta$ -galactosidase in the cell (Juers *et al.*, 2012). In addition, sucrose synthase (SUS) catalyzes the reversible conversion of sucrose and a nucleoside diphosphate into fructose and nucleotide (NDP)-glucose (Diricks *et al.*, 2015). These results suggest that *OsSte12* modulates redox homeostasis in a carbon-source-dependent manner, where glucose, fructose, and lactose induce the production of the enzymatic machinery required for sugar consumption, even when low amounts of preferred carbon sources are available.

To study sugar-metabolite related gene expression, we over-expressed these genes in the transformant *E. coli* strains containing the *OsSte12* gene under the control of the inducible *E. coli* Lac promoter. However, expressions of *LacZ* and *bglF* genes in transformants were inhibited in this plasmid, thereby lowering *LacZ* and *bglF* transcripts compared to their NT plasmids as shown in Figure 5B. Furthermore, studying gene expression in response to sugars at the level of RNA abundance can give a reliable estimate of gene activation. Figure 6 reveals that the transcriptions of sugar metabolite genes were up- or down-regulated in response to different sugar sources. In the lactose medium, highly expressed RNA levels of *LacI* and *LacY* were found in the transformants (Figure 6B), which is synergistic with the increased levels of APX, SOD, SUS, and  $\beta$ -galactosidase (Figures 3 and 4), and also exhibited a high accumulation of the 6xHis protein (Figure 1). *OsSte12* may respond to stress by up-regulating its activity and capacity of APX and SOD, and also interacts with sugar metabolites. Presumably, the accumulation of APX and SOD are favored in SUS and  $\beta$ -galactosidase, and thus help to overcome stress from sugars. Alternatively, *OsSte12* might function by modulating SUS and  $\beta$ -galactosidase as mediated by the interaction with lactose, followed by enhancing APX and SOD activity for stress tolerance. However, GR activities were much less affected in transformants under all sugar treatments. Furthermore, *LacZ* gene expression in transformed *E. coli* was reduced in the lactose medium compared to NT (Figure 6B). The reprogramming of sugar-responsive gene expressions under various sugar media reveals putative changes in metabolic pathways and enzyme activities. The functional categories of genes up-regulated

in the *OsSte12*-overexpressing of *E. coli* may be indicative of the actions of such mechanisms in stress tolerance and sugar metabolism in *E. coli*. Additionally, *OsSte12* shows higher similarity with both *A. alternata* (99%) and *L. maculans* (79%) fungi (Appendix F4). Fungus *A. alternata* not only causes leaf spots, rots, and blights on plant tissues, but also is a postharvest disease in various crops and human upper respiratory tract infections and asthma (Woudenberg *et al.*, 2015; Li *et al.*, 2023). Moreover, *L. maculans* is a fungal pathogen of the phylum Ascomycota, and is the causal agent of blackleg disease on *Brassica* crops (Howlett *et al.*, 2001). These results suggest that *OsSte12* is involved in pathogenic diseases resistance in which APX, SOD, SUS, and  $\beta$ -galactosidase might play diverse roles in resistance to various pathogenic diseases. How APX, SOD, SUS, and  $\beta$ -galactosidase are functionally connected to leaf spot, rots, and postharvest disease in crops is worthy of study.

In yeast, glucose negatively regulates the expression of genes involved in the metabolism of alternative carbon sources (Kim *et al.*, 2004a). In our study, plasmids over-expressing *Ste12* were transformed into *E. coli* cells and transformants grown in various sugar media. All sugar substrates significantly triggered *Ste12* transcription in transformants compared to NTs, and lactose is the most important transcription inducer for growing transformed *E. coli* strain compared to other substrates (Figure 7), indicating that *OsSte12* is regulated and transduced by various sugars. It is possible that enhanced cell growth is an outcome of the efficient utilization of lactose attributed to the over-expression of *Lac* in the transformed *E. coli* strain. Sugar sources, especially lactose, may be nutritional signals for activating *OsSte12*-strain growth and over-expressions of *LacI*, *LacY*, *FruB*, and *FruK* genes. Although bacteria do not possess eukaryotic-type transcription factors such as *Ste12*, functionally analogous systems exist. For example, response regulators like *OmpR*, *PhoB*, and repressors such as *LacI* integrate environmental signals and control gene expression, albeit through structurally distinct mechanisms. Furthermore, two-component systems in bacteria serve as a modular framework for signal sensing and gene regulation, functionally resembling the MAPK-transcription factor cascades in eukaryotes (Stock *et al.*, 2000; Lewis 2005; Gao *et al.*, 2009). It is worthy to conduct further studies to investigate whether *OsSte12* binds to bacterial DNA, interacts with specific operons (eg. *LacI*) or influences transcriptional regulation via conserved motifs (eg. *OmpR* and *PhoB*).

The *Ros/MucR* family which binds AT-rich DNA motifs and regulate virulence, symbiotic, and stress response genes (Janczarek *et al.*, 2022), and their ability to bind DNA was through zinc fingers (Malgieri *et al.*, 2015). In the study, we show a structural and comparative approach for hypothesizing *OsSte12*'s potential as a transcriptional regulator in a bacterial system (Table 2). While the first domain of *OsSte12* appears more divergent, possibly reflecting plant-specific neofunctionalization (e.g., hormone or developmental signaling), the second domain's homology with bacterial regulators suggests evolutionary convergence driven by similar functional pressures - nucleic acid interaction and transcriptional control. These properties are consistent with the predicted domains in *OsSte12*, suggesting potential regulatory function as expressed heterologously. The lactose-induced response is likely mediated through the *Lac* operon and associated metabolic signals, which may facilitate *OsSte12* interaction with AT-rich promoter regions resembling sugar-responsive elements (TATCCA and TGAAAC-like motifs). The partial homology of *OsSte12*'s zinc finger domains to *Ros*-like proteins implies that it may retain similar DNA-binding capacity, particularly in AT-rich contexts. Subramanian *et al.* (2024) reported that heterologously expressed plant TFs can regulate bacterial oxidative stress responses and metabolism under specific substrates. *OsSte12* functions as a eukaryotic C2H2-type regulator capable of modulating prokaryotic transcriptional and enzymatic networks under favorable carbon-source conditions. More functional assays, such as transcriptome-wide or proteomic profiling, are currently under planning for future studies. Moreover, the recognition code for C2H2 zinc fingers, as discussed in Zhang *et al.* (2024), provides a testable framework for computational binding prediction and future reporter assay design.

Functional links among sugar responses regulating adversity, enzyme activity, and sugar metabolic gene expression involved in sugar signaling transduction provide new insights into the mechanisms of physiological

relevance in *OsSte12* transformed *E. coli*. Appendix shows the expression levels of sugar metabolism factors, antioxidants, and sugar metabolism enzymes of *OsSte12* compared to the non-transformed strain. *Kluyveromyces lactis* can absorb lactose and convert it into lactic acid and has been industrially used for lactose fermentation. Liu *et al.* (2016) and Turner *et al.* (2017) over-expressed *LacZ* encoding  $\beta$ -galactosidase in the recombinant yeast strains that enables *Saccharomyces cerevisiae* to ferment lactose and produce ethanol and whey as a by-product of fermentation for the commercial markets. In our study, *OsSte12* enhanced  $\beta$ -galactosidase activity in *E. coli*, and plasmid constructions with the Lac operon will be transformed into the W3S. *cerevisiae* strain, potentially enabling it to ferment lactose. Further observations will focus on whether the transgenic strain shows increases in bioethanol yield and whey production during lactose fermentation.

## Conclusion

The functions of *OsSte12* and the sugar metabolite network were investigated in relation to growth rate, enzyme activity, and RNA level. *OsSte12* responses to various sugars were activated through signal transduction cascades involved in enzyme activity and RNA level. The over-expression of *OsSte12* transformants in lactose efficiently regulated the activity of APX, SOD, SUS, and  $\beta$ -galactosidase compared to NT, exhibiting unique abilities and specificities in response to active stressing and sugar regulation. The functional analysis of *OsSte12* genes may be useful for improving stress tolerance, facilitate our comprehension of sugar response mechanisms in *E. coli*, and is of importance for industrial events.

## Authors' Contributions

Conceptualization: KHL, CMC; Data curation: CMC, CCC, SFP; Formal analysis: CCC, SFP, YTL, MTP; Funding acquisition: CMC; Investigation: CCC, SFP; Methodology: YTL, MTP; Project administration: KHL, CMC; Resources: CMC, CCC; Software: SFP, YTL, MTP; Supervision: KHL, CMC, SFP; Validation: KHL, CMC; Visualization: CMC, CCC, SFP; Roles/Writing - original draft and Writing - review & editing: KHL, CMC.

All authors read and approved the final manuscript.

## Acknowledgements

This research received no specific grant from any funding agency in the public, commercial, or not-for-profit sectors.

## Conflict of Interests

The authors declare that there are no conflicts of interest related to this article.

## References

- Aidelberg G, Towbin BD, Rothschild D, Dekel E, Bren A, Alon U (2014). Hierarchy of non-glucose sugars in *Escherichia coli*. BMC System Biology 8:133. <https://doi.org/10.1186/s12918-014-0133-z>
- Altschul SF, Madden TL, Schäffer AA, Zhang J, Zhang Z, Miller W, Lipman DJ (1997). Gapped BLAST and PSI-BLAST: a new generation of protein database search programs. Nucleic Acids Research 25(17):3389-3402. <https://doi.org/10.1093/nar/25.17.3389>
- Asunción García-Sánchez M, Martín-Rodriguez N, Ramos B, de Vega-Bartol JJ, Perlin MH, Díaz-Mínguez JM (2010). Fost12, the *Fusarium oxysporum* homolog of the transcription factor Ste12, is upregulated during plant infection and required for virulence. Fungal Genetic Biology 47:216-225. <https://doi.org/10.1016/j.fgb.2009.11.006>
- Bernaerts M, De Ley J (1963). A biochemical test for crown gall bacteria. Nature 197:406-407. <https://doi.org/10.1038/197406b0>
- Bouhouche N, Syvanen M, Kado CI (2000). The origin of prokaryotic C2H2 zinc finger regulators. Trends in Microbiology 8(2):77-81. [https://doi.org/10.1016/s0966-842x\(99\)01679-0](https://doi.org/10.1016/s0966-842x(99)01679-0)
- Bustin SA, Benes V, Garson JA, Hellemans J, Huggett J, Kubista M, ... Wittwer CT (2009). The MIQE guidelines: minimum information for publication of quantitative real-time PCR experiments. Clinical Chemistry 55(4):611-22. <https://doi.org/10.1373/clinchem.2008.112797>
- D'Ambrosca G, Paladino A, Baglivo I, Russo L, Sassano M, Grazioso R, ... Malgieri G (2020). Structural insight of the full-length Ros protein: A prototype of the prokaryotic zinc-finger family. Scientific Reports 10(1):9283. <https://doi.org/10.1038/s41598-020-66204-5>
- Diricks M, De Bruyn F, Van Daele P, Walmagh M, Desmet T (2015). Identification of sucrose synthase in nonphotosynthetic bacteria and characterization of the recombinant enzymes. Applied Microbiology and Biotechnology 99(20):8465-8474. <https://doi.org/10.1007/s00253-015-6548-7>
- Elion E, Qi M, Chen W (2005). Signaling specificity in yeast. Science 307:687-688. <https://doi.org/10.1126/science.1109500>
- Engström-Öst J, Glippa O, Feely RA, Kanerva M, Keister JE, Alin SR, Carter BR, McLaskey AK, Vuori KA, Bednarek N (2019). Eco-physiological responses of copepods and pteropods to ocean warming and acidification. Scientific Reports 9(1):4748. <https://doi.org/10.1038/s41598-019-41213-1>
- Esposito S, Ilaria B, Gaetano M, Luigi R, Laura Z, Luca D, D'A, Marco M, Benedetto DB, Carla I, Roberto F, Paolo V (2006). A novel type of zinc finger DNA binding domain in the *Agrobacterium tumefaciens* transcriptional regulator Ros. Biochemistry 45(34):10394-10405. <https://doi.org/10.1021/bi060697m>
- Gao R, Stock AM (2009). Biological insights from structures of two-component proteins. Annual Review of Microbiology 63:133-154. <https://doi.org/10.1146/annurev.micro.091208.073214>
- Garg SG, Hochberg GK (2025). A general substitution matrix for structural phylogenetics, capturing remote homology. Molecular Biology and Evolution 42(6):124. <https://doi.org/10.1093/molbev/msaf124>
- Gomes MP, Kitamura RS, Marques RZ, Barbato ML, Zamocky M (2022). The role of H<sub>2</sub>O<sub>2</sub>-scavenging enzymes (ascorbate peroxidase and catalase) in the tolerance of Lemna minor to antibiotics: Implications for phytoremediation. Antioxidants (Basel) 11(1):151. <https://doi.org/10.3390/antiox11010151>
- Gu Q, Zhang C, Liu X, Ma Z (2015). A transcription factor FgSte12 is required for pathogenicity in *Fusarium graminearum*. Molecular Plant Pathology 16:1-13. <https://doi.org/10.1111/mpp.12155>
- Gruber S, Zeilinger S (2014). The transcription factor Ste12 mediates the regulatory role of the Tmk1 MAP kinase in mycoparasitism and vegetative hyphal fusion in the filamentous fungus *Trichoderma atroviride*. PLoS One 9:e111636. <https://doi.org/10.1371/journal.pone.0111636>
- Hamamsy T, Morton JT, Blackwell R, Berenberg D, Carriero N, Gligorijevic V, ... Bonneau R (2024). Protein remote homology detection and structural alignment using deep learning. Nature Biotechnology 42(6):975-985. <https://doi.org/10.1038/s41587-023-01917-2>
- Hemmadi V (2016). Metallothionein- A potential biomarker to assess the metal contamination in marine fishes- A review. International Journal of Bioassays 5(4):4961-4973. <https://doi.org/10.21746/ijbio.2016.04.003>
- Hoi WS, Dumas B (2010). Ste12 and Ste12-like proteins, fungal transcription factors regulating development and pathogenicity. Eukaryote Cell 9: 480-485. <https://doi.org/10.1128/ec.00333-09>

- Howlett BJ, Idnurm A, Pedras MS (2001). *Leptosphaeria maculans*, the causal agent of blackleg disease of Brassicas. *Fungal Genetics and Biology* 33(1):1-14. <https://doi.org/10.1006/jfghi.2001.1274>
- Janczarek M (2022). The Ros/MucR zinc-finger protein family in bacteria: Structure and functions. *International Journal of Molecular Science* 23:15536. <https://doi.org/10.3390/ijms232415536>
- Jia H, Zhou Q, Li P, Li M, Li X, Liu Z, Gong X, Dong J, Gu S, Liu Y (2025). Characterization of the C2H2 zinc finger protein family in *Setosphaeria turcica*. *Agronomy* 15(6):1434. <https://doi.org/10.3390/agronomy15061434>
- Juers DH, Matthews BW, Huber RE (2012). LacZ  $\beta$ -galactosidase: structure and function of an enzyme of historical and molecular biological importance. *Protein Science* 21(12):1792-807. <https://doi.org/10.1002/pro.2165>
- Kim TS, Hye YK, Jin HY, Hyen SK (2004a). Recruitment of the Swi/Snf complex by Ste12-Tec1 promotes Flo8-Mss11-mediated activation of *STAI* expression. *Molecular Cellular Biology* 24:9542-9556. <https://doi.org/10.1128/MCB.24.21.9542-9556.2004>
- Kim TS, Sung BL, Hyen SK (2004b). Glucose repression of *STAI* expression is mediated by the Nrg1 and Sfl1 repressors and the Srb8-11 complex. *Molecular Cellular Biology* 24:7695-7706. <https://doi.org/10.1128/MCB.24.17.7695-7706.2004>
- Lang, TJ, Brodsky S, Manadre W, Vidavski M, Valinsky G, Mindel V, Ilan G, Carmi M, Jonas F, Barkai N (2024). Massively parallel binding assay (MPBA) reveals limited transcription factor binding cooperativity, challenging models of specificity. *Nucleic Acids Research* 52(20):12227-12243. <https://doi.org/10.1093/nar/gkac846>
- Larkin MA, Blackshields G, Brown NP, Chenna R, McGettigan PA, McWilliam H, ... Higgins DG (2007). Cluster W and Cluster X version 2.0. *Bioinformatics* 23:2947-2948. <https://doi.org/10.1093/bioinformatics/btm404>
- Lewis M (2005) The lac repressor. *Comptes Rendus Biologies* 328(6):521-548. <https://doi.org/10.1016/j.crv.2005.04.004>
- Liu JJ, Zhang GC, Oh EJ, Pathanibul P, Turner TL, Jin YS (2016). Lactose fermentation by engineered *Saccharomyces cerevisiae* capable of fermenting cellobiose. *Journal of Biotechnology* 234:99-104. <https://doi.org/10.1016/j.jbiotec.2016.07.018>
- Li W, Huang W, Zhou J, Wang J, Liu J, Li Y (2023). Evaluation and control of *Alternaria alternata* causing leaf spot in soybean in Northeast China. *Journal of Applied Microbiology* 16:134. <https://doi.org/10.1093/jambio/lxad004>
- Lin KH, Sei SC, Su YH, Chiang CM (2019). Overexpression of the *Arabidopsis* and winter squash superoxide dismutase genes enhances chilling tolerance via ABA-sensitive transcriptional regulation in transgenic *Arabidopsis*. *Plant Signal Behavior* 14(12):1685728. <https://doi.org/10.1080/15592324.2019.1685728>
- Liu L, Ji Z, Zhao K, Zhao Y, Zhang Y, Huang S (2022). Validation of housekeeping genes as internal controls for gene expression studies on biofilm formation in *Bacillus velezensis*. *Applied Microbiology and Biotechnology* 106(5):2079-2089. <https://doi.org/10.1007/s00253-022-11831-3>
- Lu CA, Lim EK, Yu SM (1998). Sugar response sequence in the promoter of a rice alpha-amylase gene serves as a transcriptional enhancer. *Journal of Biological Chemistry* 273: 10120-10131. <https://doi.org/10.1074/jbc.273.17.10120>
- Lu CA, Ho T-H D, Ho SL, Yu SM (2002). Three novel MYB proteins with one DNA binding repeat mediate sugar and hormone regulation of  $\alpha$ -amylase gene expression. *The Plant Cell* 14: 1963-1980. <https://doi.org/10.1105/tpc.001735>
- Lu L, Xiao M, Xu X, Li Z, Li Y (2007). A novel beta-galactosidase capable of glycosyl transfer from *Enterobacter agglomerans* B1. *Biochemical and Biophysical Research Communications* 27:356(1):78-84. <https://doi.org/10.1016/j.bbrc.2007.02.106>
- Lyu X, Wang Q, Liu A, Liu F, Meng L, Wang P, Zhang Y, Wang L, Li Z, Wang W (2023). The transcription factor Ste12-like increases the mycelial abiotic stress tolerance and regulates the fruiting body development of *Flammulina filiformis*. *Frontier Microbiology* 14:1139679. <https://doi.org/10.3389/fmicb.2023.1139679>
- Madhani HD, Fink GR (1997). Combinatorial control required for the specificity of yeast MAPK signaling. *Science* 275:1314-1317. <https://doi.org/10.1126/science.275.5304.1314>
- Malgieri G, Luigi R, Sabrina E, Ilaria B, Laura Z, Emilia MP, Benedetto DB, Carla I, Paolo VP, Roberto F (2007). The prokaryotic Cys2His2 zinc-finger adopts a novel fold as revealed by the NMR structure of *Agrobacterium tumefaciens* Ros DNA-binding domain. *PNAS* 104:17341-17346. <https://doi.org/10.1073/pnas.0706659104>

- Malgieri G, Palmieri M, Russo L, Fattorusso R, Pedone PV, Isernia C (2015). The prokaryotic zinc-finger: structure, function and comparison with the eukaryotic counterpart. *The FEBS Journal* 282(23):4480-4496. <https://doi.org/10.1111/febs.13503>
- Merlini L, Dudin O, Martin SG (2013). Mate and fuse: how yeast cells do it. *Open Biology* 3:130008. <https://doi.org/10.1098/rsob.130008>
- Pinheiro S, Nadal-Ribelles M, Solé C, Vincenzetti V, Dusserre Y, Posas F, Pelet S (2025). Basal association of a transcription factor favors early gene expression. *PLoS Genetics* 21(6):e1011710. <https://doi.org/10.1371/journal.pgen.10117>
- Record MT, Courtenay DS, Guttman HJ (1998). Responses of *E. coli* to osmotic stress: large changes in amounts of cytoplasmic solutes and water. *TIBS* 23 (4):143-148. [https://doi.org/10.1016/S0968-0004\(98\)01196-7](https://doi.org/10.1016/S0968-0004(98)01196-7)
- Remmert M, Biegert A, Hauser A, Söding J (2012). HHblits: Lightning-fast iterative protein sequence searching by HMM-HMM alignment. *Nature Methods* 9(2):173-175. <https://doi.org/10.1038/nmeth.1818>
- Ren R, Yue X, Li J, Xie S, Guo S, Zhang Z (2020). Coexpression of sucrose synthase and the SWEET transporter, which are associated with sugar hydrolysis and transport, respectively, increases the hexose content in *Vitis vinifera* L. grape berries. *Frontier Plant Science* 11:321. <https://doi.org/10.3389/fpls.2020.00321>
- Rispail N, Di Pietro A (2010). The homeodomain transcription factor Ste12: Connecting fungal MAPK signaling to plant pathogenicity. *Communicative and Integrative Biology* 3:327-332. <https://doi.org/10.4161/cib.3.4.11908>
- Schalamun M, Hinterdobler W, Schinnerl J, Brecker L, Schmoll M (2024). The transcription factor STE12 influences growth on several carbon sources and production of dehydroacetic acid (DHAA) in *Trichoderma reesei*. *Scientific Report* 14(1):9625. <https://doi.org/10.1038/s41598-024-59511-8.5>
- Schneider CA, Rasband WS, Eliceiri KW (2012). NIH Image to ImageJ: 25 years of image analysis. *Natural Methods* 9(7):671-5. <https://doi.org/10.1038/nmeth.2089>
- Sezonov G, Joseleau-Petit D, D'Ari R (2007). *Escherichia coli* physiology in Luria-Bertani broth. *Journal of bacteriology* 189(23):8746-8749. <https://doi.org/10.1128/jb.01368-07>
- Stock AM, Robinson VL, Goudreau PN (2000). Two-component signal transduction. *Annual Review of Biochemistry* 69:183-215. <https://doi.org/10.1146/annurev.biochem.69.1.183>
- Subramanian R, Pandi NU, Thangavel R, Swamy LR, Lakshminarayanan SP, Santham S, Ravalan BM, Jacob R (2024). Functional validation of mungbean LEA protein coding gene in bacterial expression system confers salt stress tolerance. *Notulae Botanicae Horti Agrobotanici Cluj-Napoca* 52(3):13416. <https://doi.org/10.15835/nbha52313416>
- Taylor S, Wakem M, Dijkman G, Alsarraj M, Nguyen M (2010). A practical approach to RT-qPCR-Publishing data that conform to the MIQE guidelines. *Methods* 50(4):S1-S5. <https://doi.org/10.1016/j.ymeth.2010.01.005>
- Tamura K, Stecher G, Kumar S (2021). MEGA11: Molecular evolutionary genetics analysis Version 11. *Molecular Biology* 38(7):3022-3027. <https://doi.org/10.1093/molbev/msab120>
- Tan LR, Liu JJ, Deewan A, Lee JW, Xia PF, Rao CV, Jin YS, Wang SG (2022). Genome-wide transcriptional regulation in *Saccharomyces cerevisiae* in response to carbon dioxide. *FEMS Yeast Research* 22(1):foac032. <https://doi.org/10.1093/femsyr/foac032>
- Turner TL, Kim E, Hwang C, Zhang GC, Liu JJ, Jin YS (2017). Short communication: Conversion of lactose and whey into lactic acid by engineered yeast. *Journal of Dairy Science* 100(1):124-128. <https://doi.org/10.3168/jds.2016-11784>
- Vargas WA, Pontis HG, Salerno GL (2008). New insights on sucrose metabolism: evidence for an active A/N-Inv in chloroplasts uncovers a novel component of the intracellular carbon trafficking. *Planta* 227(4):795-807. <https://doi.org/10.1007/s00425-007-0657-1>
- Wong Sak Hoi J, Dumas B (2010). Ste12 and Ste12-like proteins, fungal transcription factors regulating development and pathogenicity. *Eukaryote Cell* 9(4):480-485. <https://doi.org/10.1128/EC.00333-09>
- Wei QL, Du YR, Jin K, Xia YX (2017). The Ste12-like transcription factor MaSte12 is involved in pathogenicity by regulating the appressorium formation in the entomopathogenic fungus, *Metarhizium acridum*. *Applied Microbiology and Biotechnology* 101:8571–8584. <https://doi.org/10.1007/s00253-0178>

- Woudenberg JH, Seidl MF, Groenewald JZ, de Vries M, Stielow JB, Thomma BP, Crous PW (2015). *Alternaria* section *Alternaria*: Species, formae speciales or pathotypes? Study in Mycology 82:1-21. <https://doi.org/10.1016/j.simyco.2015.07.001>
- Yu L, Yang Y, Qiu X, Xiong D, Tian C (2024). The mitogen-activated protein kinase module CcSte11-CcSte7-CcPmk1 regulates pathogenicity via the transcription factor CcSte12 in *Cytospora chrysosperma*. Stress Biology 4(1):4. <https://doi.org/10.1007/s44154-023-00142-w>
- Yu L, Yang Y, Xiong D, Tian C (2022). Phosphoproteomic and meta bolomic profiling uncovers the roles of CcPmk1 in the pathogenicity of *Cytospora chrysosperma*. Microbiology Spectrum 10:e0017622. <https://doi.org/10.1128/spectrum.00176-22>
- Zhang X, Blumenthal RM, Cheng X (2024). Updated understanding of the protein–DNA recognition code used by C2H2 zinc finger proteins. Current Opinion in Structural Biology 87:102836. <https://doi.org/10.1016/j.sbi.2024.102836>

## Appendix

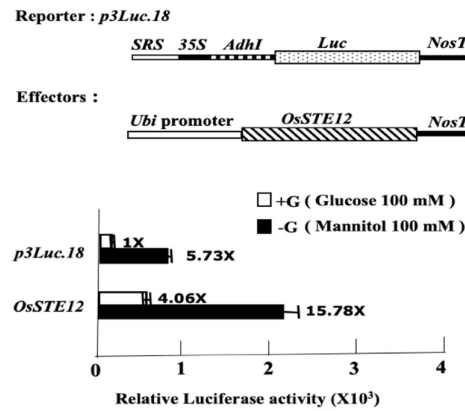


**Figure A1.** The function of *OsSte12* in sugar regulation of  $\alpha$ -amylase3 (*a-Amy3*) gene expression using the rice embryo transient expression assay

*OsSte12* was required for sugar starvation induced sugar response sequence (SRS) promoter activity from -186 to -82 relative to the transcription start site of *a-Amy3* (Lu *et al.*, 1998). The SRS was fused upstream of the *CaMV35S* (35S) minimal promoter-*Luc* chimeric gene and used as a reporter construct p3Luc.18. *OsSte12* was then fused downstream of the maize ubiquitin gene (*Ubi*) promoter and used as an effector construct (Lu *et al.*, 2002). The rice embryos were then particle bombarded simultaneously with the effector and reporter plasmids, divided into two halves, and each half was incubated with 100mM glucose (+G) or without glucose but with 100mM mannitol (-G) for 18 h, and luciferase activity was determined. Overexpression *OsSte12* increased luciferase activity in the absence of glucose (-G) group. Thus, *OsSte12* was required for sugar starvation induced SRS promoter activity (Lu *et al.*, 1998; Lu *et al.*, 2002)

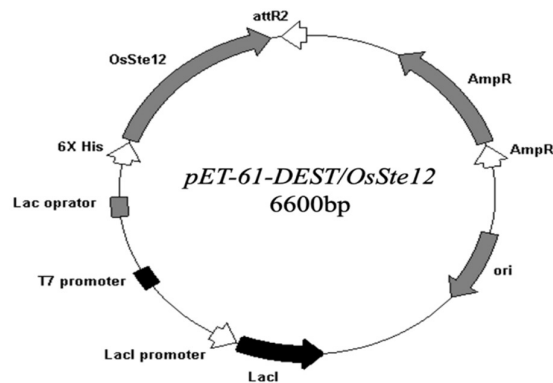


**Figure A2.** Vector map of pET-61-DEST/*OsSte12*

As described in the *Materials and Methods* section, the recombinant construct was generated by cloning *OsSte12* cDNA (1,260 bp, accession AK110102) into the pET-61-DEST destination vector (NovoPro Bioscience, China) using the Gateway™ LR Clonase system. For heterologous expression analyses, *E. coli* DH5 $\alpha$  (F<sup>-</sup>  $\phi$ 80 lacZ $\Delta$ M15  $\Delta$  [lacZYA-argF] U169 recA1 endA1 hsdR17 [rK<sup>-</sup>mK<sup>+</sup>] phoA supE44 thi-1 gyrA96 relA1  $\lambda$ <sup>-</sup>) was employed for high-efficiency plasmid maintenance and amplification of both entry and destination vectors. The verified construct was introduced into *E. coli* BL21 (DE3) for expression under the IPTG-inducible T7 promoter. The expression host *E. coli* BL21 (DE3) [pET-61-DEST] (F<sup>-</sup> ompT hsd SB [rB<sup>-</sup>mB<sup>-</sup>] gal dcm; DE3 lysogen carrying T7 RNA polymerase; Amp<sup>R</sup>) served as the vector-only, non-transformant (NT) control to establish baseline growth, enzyme activity, and gene expression levels. The recombinant strain *E. coli* BL21 (DE3) [pET-61-DEST/*OsSte12*], carrying the *OsSte12* cDNA under the T7 promoter, expressed a His-tagged 43 kDa *OsSte12* protein. This transformant was used to

evaluate the functional effects of *OsSte12* on antioxidant enzyme activities (APX, SOD, and GR), sugar-metabolite gene expression, and carbon-source-dependent metabolic regulation. All constructs were confirmed by PCR and sequencing, and His-*OsSte12* expression was verified by Western blotting (Figure 1). Both the vector-only and *OsSte12*-expressing strains were cultivated under identical conditions in LB or sugar-specific minimal media (glucose, sucrose, fructose, lactose, and mannitol). Amp<sup>R</sup> indicates the ampicillin-resistance marker used for plasmid selection

OsSte12 1	<u>MSMPPSMQNTVVKSREHRELSQSFQYDRNGIPLSQVHORHSSMPAYMEYSPAPSFVSSHY</u>	60
AaSte 277	<u>MSMPPSMQNTVVKSREHRELSQSFQYDRNGIPLSQVHORHSSMPAYMEYSPAPSFVSSHY</u>	336
OsSte12 61	<u>EDYSTRGMSFEPLTPPQHQIIGLGAEPAYIANEDTGLYSAIPDLVPNTFNPLMNPSSNL</u>	120
AaSte 337	<u>EDYSTRGMSFEPLTPPQHQIIGLGAEPAYIANEDTGLYSAIPDLVPNTFNPLMNPSSNL</u>	396
OsSte12 121	<u>MGSYGPVSRPFAPGNVYSVIEGSPTYKQRRRRSSL SAGAAAVTASGAGAHQVHRPSDL</u>	180
AaSte 397	<u>MGSYGPVSRPFAPGNVYSVIEGSPTYKQRRRRSSL SAGAAAVTASGAGAHQVHRPSDL</u>	456
OsSte12 181	<u>RRSMSSSVVPLAEVDESNNHNSPNSQNGTSYPQMPEAKPHLDMSRQGTPLNTVEESPEPQS</u>	240
AaSte 457	<u>RRSMSSSVVPLAEVDESNNHNSPNSQNGTSYPQMPEAKPHLDMSRQGTPLNTVEESPEPQS</u>	516
OsSte12 241	<u>ASLHHDDLNTLVNGELFESPLQHSAVARTAGAGPVFRRARSATMMEIGYPYQKPHSCPIP</u>	300
AaSte 517	<u>ASLHHDDLNTLVNGELFESPLQHSAVARTAGAGPVFRRARSATMMEIGYPYQKPHSCPIP</u>	576
OsSte12 301	<u>TCGRLFKRLEHLKRHVTRHTQERPYVCP LCNKAFSRSDNLAQHRRTHEPRADGEPLSDYQ</u>	360
AaSte 577	<u>TCGRLFKRLEHLKRHVTRHTQERPYVCP LCNKAFSRSDNLAQHRRTHEPRADGEPLSDYQ</u>	636
OsSte12 361	<u>DEEDLEGEDDHLNSLQDELSPESGNEYLGLSHSINDIPGRLGMTAPPQSLMAASHY</u>	419
AaSte 637	<u>DEEDLEGEDDHLNSLQDELSPESGNEYLGLSHSINDIPGRLGMTAPPQSLMAASHY</u>	695

**Figure A3.** Comparisons of amino acid sequences between *Oryza sativa* (*Os*) *Ste12* (AK\_110102.1) and *Alternaria alternate* *Ste* (XM\_018535684.1)

Open-reading frame sequences (shown in the underline of amino acid sequences) of both species' identities by 413/419 (99%) base pairs

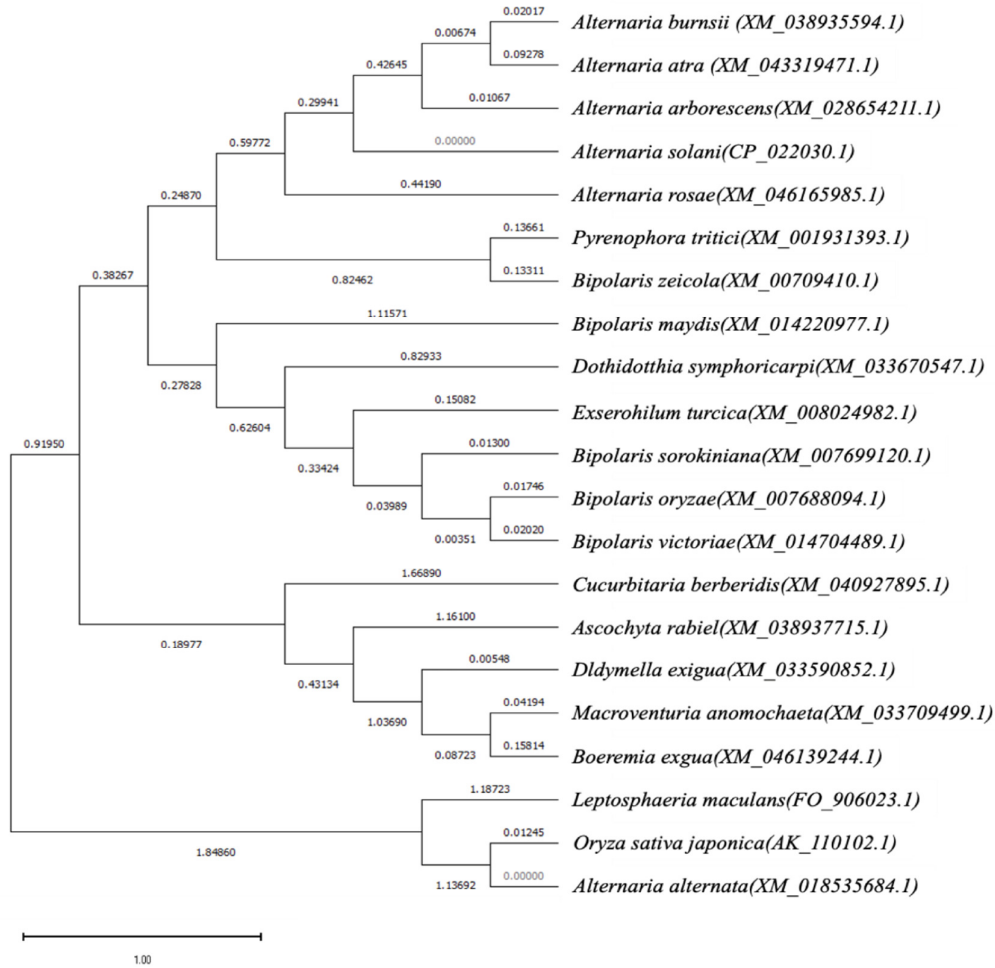


**Figure A4.** Phylogenetic tree analysis inferred from Ste12 protein sequences by the Neighbor-Joining method

Numbers indicate bootstrap support for individual nodes. The scale at the bottom shows the number of substitutions per amino acid site. GenBank accession number is indicated after the species name

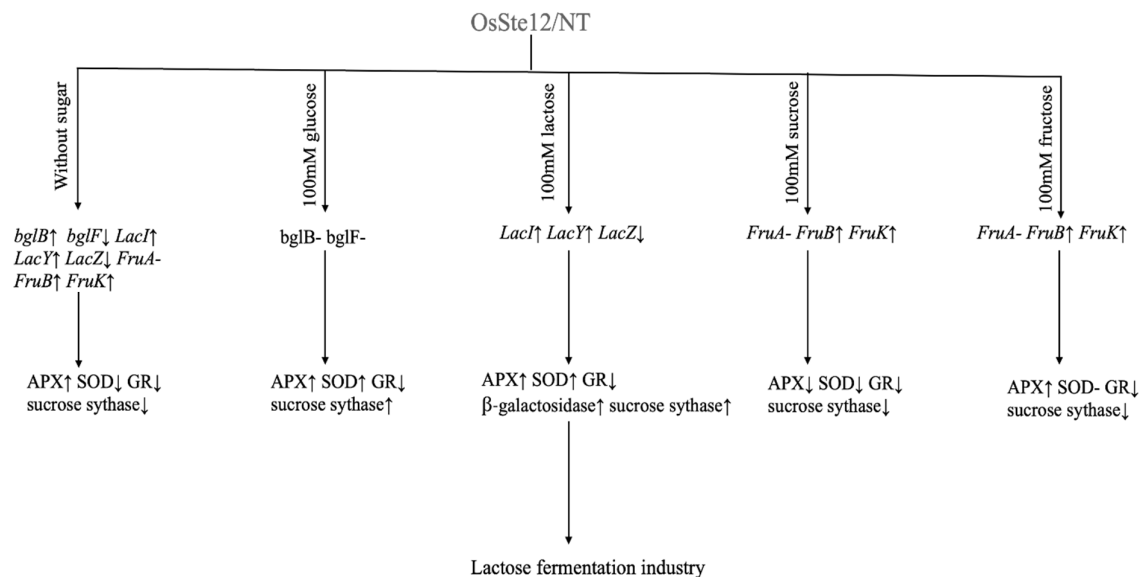


**Figure A5.** The expression levels of sugar metabolism factors, antioxidants, and sugar metabolism enzymes in *OsSte12* compared to the non-transformed strain are presented graphically

Where ↑ indicates an increase in expression or activity, ↓ indicates a decrease in expression or activity, and – indicates no significant difference. In the study, *OsSte12* enhanced β-galactosidase activity in *E. coli*, and plasmid constructions with the Lac operon will be transformed into the W3*S. cerevisiae* strain, potentially increasing lactose fermentation in the transgenic strain



The journal offers free, immediate, and unrestricted access to peer-reviewed research and scholarly work. Users are allowed to read, download, copy, distribute, print, search, or link to the full texts of the articles, or use them for any other lawful purpose, without asking prior permission from the publisher or the author.



**License** -Articles published in *Notulae Botanicae Horti Agrobotanici Cluj-Napoca* are Open-Access, distributed under the terms and conditions of the Creative Commons Attribution (CC BY 4.0) License.

© Articles by the authors; Licensee UASVM and SHST, Cluj-Napoca, Romania. The journal allows the author(s) to hold the copyright/to retain publishing rights without restriction.

**Notes:**

- **Material disclaimer:** The authors are fully responsible for their work and they hold sole responsibility for the articles published in the journal.
- **Maps and affiliations:** The publisher stay neutral with regard to jurisdictional claims in published maps and institutional affiliations.
- **Responsibilities:** The editors, editorial board and publisher do not assume any responsibility for the article's contents and for the authors' views expressed in their contributions. The statements and opinions published represent the views of the authors or persons to whom they are credited. Publication of research information does not constitute a recommendation or endorsement of products involved.